Characterization of III-V Semiconductor Structures Using Electron Beam Electroreflectance (EBER) Spectroscopy

M.H. Herman, I.D. Ward,
S.E. Buttrill, Jr., and
G.L. Francke

MRS PROCEEDINGS REPRINT

CHARLES EVANS & ASSOCIATES
SPECIALISTS IN MATERIALS CHARACTERIZATION

Reprinted from Materials Research Society Symposium Proceedings Volume 144, *Advances in Materials, Processing and Devices in III-V Compound Semiconductors*, D.K. Sadana, L. Eastman and R. Dupuis, editors.

CHARACTERIZATION OF III-V SEMICONDUCTOR STRUCTURES USING ELECTRON BEAM ELECTROREFLECTANCE (EBER) SPECTROSCOPY.

M. H. HERMAN, I. D. WARD, S. E. BUTTRILL, JR., AND G. L. FRANCKE
Charles Evans & Associates, 301 Chesapeake Drive, Redwood City, CA 94063

ABSTRACT

EBER is a form of modulated reflectance spectroscopy in which a low energy electron beam alters the sample surface potential. For III-V semiconductors, the spectra are characteristic of electroreflectance, including excitonic, interband, and impurity transitions. The study of these transitions provides accurate estimations of band gaps in bulk and thick film samples. Measurements of the band gap energy in compounds such as $Al_xGa_{1-x}As$ provide highly precise evaluations of their composition.

Additionally, EBER spectra of quantum well structures and heterojunctions provide useful information about the composition and quality of materials and interfaces. For quantum wells, detected features suggest the presence of allowed, disallowed, and resonant states. In EBER spectra of HEMT structures, peaks are apparent resulting from transitions between the valence band and the states in which the electrons are confined. We present examples of EBER determination of AlGaAs composition, single GaAs/AlGaAs quantum well evaluation, and HEMT characterization.

INTRODUCTION

For studies of the electronic structure of crystalline materials, modulation spectroscopies [1] have been widely employed [2]. These techniques have the capability to measure the optical band gaps, impurity levels [3], and excitonic transitions in solids, even for artificially structured and indirect gap materials. Recently, modulation spectroscopies have been successfully utilized for studies of bulk GaAs wafers and epi films, quantum well (QW), superlattice, and HEMT structures. Particularly in the latter case, modulation spectroscopies give clear evidence of the quantized 2-D electron gas states of HEMT structures.

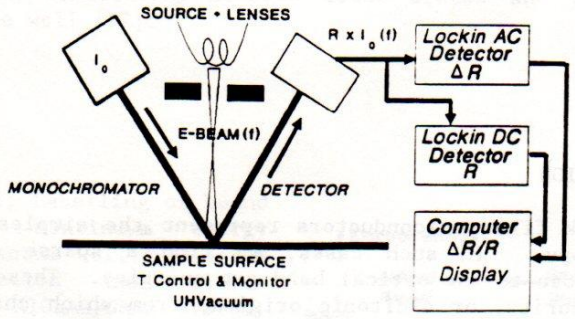

Figure 1: Schematic EBER Configuration. Monochromatic light reflects from the sample into a detector. A fraction (ΔR) of the total reflected light (R) has the same frequency (f) as the electron beam. The resulting AC and DC signal components, ΔR and R, are taken in ratio ($\Delta R/R$) for the spectrum.

EXPERIMENTAL DETAILS

To overcome weaknesses inherent in alternative non-contact methods of electroreflectance (ER) modulation spectroscopy, we have developed a novel approach. The Electron Beam Electroreflectance (EBER) spectrometer, schematically indicated in Figure 1, incorporates a low energy (240eV) electron beam to alter the surface potential of the sample. Following thermalization [4], the electron current breaks into three conceptual components, one which charges surface states, another flows across the surface, and a third which may penetrate the bulk. For low current densities, the beam causes a net negative surface charge, which provides contactless electric field modulation [5]. Thus, the surface field can be amplified as desired.

EBER therefore provides a distinct advantage over alternative non-contact ER methods such as photoreflectance (PR). The inherent strength of ER signals depends upon the square of the modulating electric field [6]. In PR, modulation is accomplished by annihilation of existing surface fields [7], limiting its utility where built-in electric fields are small or where structures lie beyond these fields [8]. Also, EBER may permit the sample carrier type to be detected from the "phase" of the spectrum. This is possible with contact methods, of ER but is impossible in PR which always reduces existing fields.

Additionally, the vacuum system required for the electron beam provides experimental advantages. Typically, analyses are performed at 5×10^{-9} torr, relieving issues of surface contamination. Thermostatically controlled cryogenic cooling, provided on our system, also facilitates studies of the temperature dependence of energy levels and line broadening. Lower temperatures also permit improved studies of excitonic effects.

Furthermore, our EBER system has the capability of fitting experimental spectra to theoretical lineshapes using non-linear least-squares algorithms. For example, interband transitions are appropriately described by a 2 or 3-dimensional, 3^{rd} derivative lineshape. Exciton lines, in contrast, are suitably matched to 0-dimensional 1st derivative lineshapes. The computerized fitting provides very accurate estimates of band gap and broadening parameters, enabling differences between samples to be sensitively ascertained.

RESULTS AND DISCUSSION

Bulk and thick film semiconductors represent the simplest application of EBER spectroscopy. In such cases, we find a sparse spectrum with features evident close to the optical band gap energies. These features may have interband, impurity, or excitonic origins, from which characterization of crystal quality and composition may be made.

As an example, we examine a sample of MBE grown $Al_xGa_{1-x}As$. This sample has a nominal x value of 0.20. Experimental and theoretical EBER spectra of this sample are shown in Figure 2. The features labelled "E_0" for the GaAs and AlGaAs are composed of bound exciton, free exciton, and interband transitions. We have matched these spectra to a single excitonic lineshape for each case [9], showing the agreement is reasonable. Least squares fitting provides an energy of 1.413 eV for the GaAs and 1.674eV for the AlGaAs for this example. Correspondingly, we estimate the value of x to be 0.197, with a σ of 0.003 from this model [10].

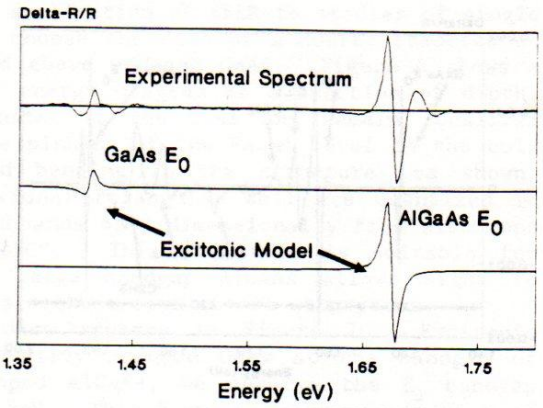

Figure 2: EBER Spectrum of x=0.20 $Al_xGa_{1-x}As$. Note that E_0 transitions from both the GaAs and the AlGaAs film are detected. Shown below the data are the fitted lineshapes, using excitonic transitions as a basis. The resulting energy gap of the AlGaAs 1.674eV, corresponds to x = 0.197 ± 0.003.

As a second example, we describe EBER analysis of bound state transitions in AlGaAs/GaAs quantum wells. An electron energy diagram for the rectangular barrier model is shown in Figure 3 for this case, indicating both bound and unbound continuum states. The electronic states of these structures have been studied by many techniques, but only in a limited number of cases have observations of forbidden transitions (Δn odd) and states above the barrier been reported [11]. We depict in Figure 4 the EBER spectrum of a 50Å well at 90K. This spectrum has labelled the major transition assignments which result from the rectangular barrier model. Note the sharp, excitonic peaks which originate from the GaAs substrate and AlGaAs barrier layers. The spectral peaks at intermediate energies result from excitonic levels associated with bound state transitions. Importantly, we observe not only the lowest allowed transitions C1H1 and C1L1, but also parity forbidden transitions such as C1H2, C2H1, and C1H3. Additional levels are also present in the spectrum, as shown in Figure 5, which we associate with transitions between bound states and the continuum lying outside of the well [12].

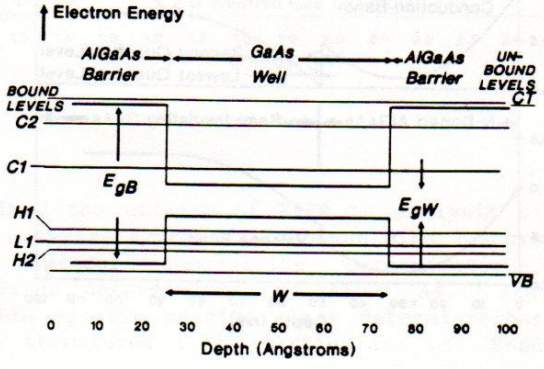

Figure 3: Labelling of bound and unbound continuum energy levels in quantum well. Diagram shows conduction and valence bands of the AlGaAs/GaAs system. Electron energy levels of the conduction band have a "C" prefix; those of the valence band are separated into light and heavy hole levels "L" and "H" respectively. The edge of the continuum levels are schematically indicated as "CT" for conduction band top, and "VB" for valence band bottom.

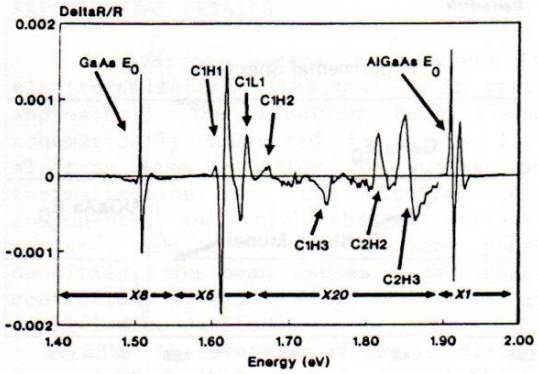

Figure 4: EBER Spectrum of a 50Å $Al_xGa_{1-x}As$/GaAs Single Quantum Well. Note that E_0 is observed from both the GaAs substrate and the AlGaAs barriers. At 90K, these band gaps appear at 1.505eV and 1.909eV. Between lie the excitonic transitions associated with the bound conduction and valence band levels. The labels are based upon the rectangular barrier model shown in Figure 3. The results of the model give a well width of 53Å.

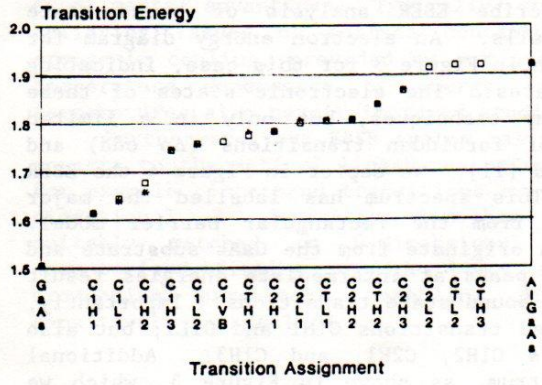

Figure 5: Match between rectangular barrier model of Figure 3 and experimental EBER peak energies of Figure 4. Both allowed (Δn even) and forbidden (Δn odd) transitions are observed. Levels near 1.9eV are obscured by the AlGaAs E_0 peak. The well width parameter of 53Å closely matches the nominal value of 50Å.

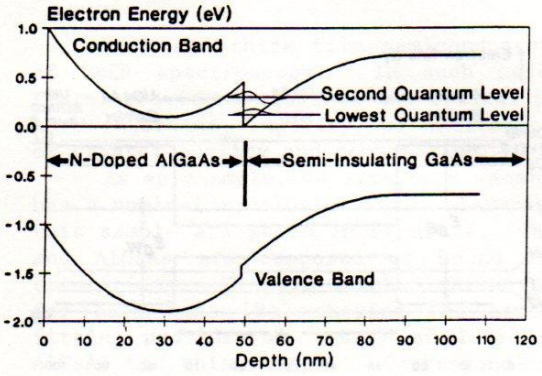

Figure 6: Electron Energy Diagram of HEMT Structure. Note that the N-doped AlGaAs layer allows light to penetrate to the 2-D electron gas and the GaAs substrate. The band bending depicted arises from Fermi level pinning at the surface and within the substrate, and from the doping of the AlGaAs.

We give as a final example the application of EBER to studies of single heterojunctions. In particular, we choose the case of a MODFET composed of N-doped AlGaAs epitaxially deposited above undoped GaAs. Figure 6 shows a schematic of this structure and its energy diagram as a function of depth. Free carriers from the AlGaAs transfer to the GaAs and remain localized there in a triangular well. Surface pinning of the Fermi level in the bulk and at the surface cause the band bending in the structure, as shown. Electron states within the 1-dimensional triangular well are quantized in energy. These energy levels form subbands of 2-dimensionally free electrons -- the "2-D electron gas," or "2DEG". This structure is suitable for optical analysis by EBER, as the large bandgap AlGaAs allows light to penetrate to the GaAs and 2DEG states without significant absorption.

The EBER spectrum for this case appears in Figure 7. Excitonic transitions appear from the high quality undoped GaAs at the bandgap of 1.424eV. Likewise, from the Si-doped AlGaAs, we observe the E_0 bandgap transition at 1.8eV and $E_0+\Delta_0$ at 2.15eV. This E_0 value corresponds to x of 0.25 for the $Al_xGa_{1-x}As$ layer, after accounting for the free carrier Burstein shift.

At intermediate energies between the GaAs E_0 and the AlGaAs E_0, lie the states of the 2D electron gas. These states have been observed by other ER techniques [13], but are not as clearly evident from PL studies [14]. Recent theoretical analysis suggests that these additional spectral features originate from transitions between valence band Bloch states and the wavefunctions of the 2DEG [15]. The free n=1 exciton has an ionization field of about 5×10^5 V/m in bulk GaAs, so at first excitonic effects seem unimportant due to the known high fields (10^7 V/m) present at the heterojunction interface of a HEMT. However, excitonic contributions cannot be completely ruled out, due to the effects of electron confinement at the interface. This confinement increases the exciton Rydberg by a factor of 6.2 [16], and enhances the ionization field by nearly 38, to 2×10^7 V/m.

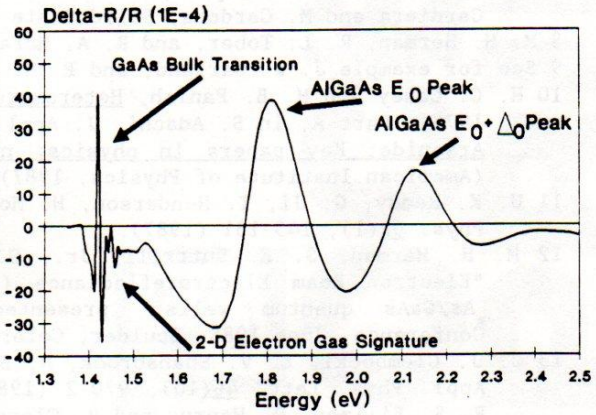

Figure 7: EBER Spectrum of HEMT Structure. Note that E_0 signals are observed from both the N-doped AlGaAs layer and the GaAs substrate. Just above the GaAs exciton peak are features attributable to the 2-D electron gas.

CONCLUSION

In this paper, we have described the utility of EBER to analysis of exemplary III-V bulk and structured material systems. We began with a short discussion of applications to optical composition determinations, specifically demonstrating the x-value determination of $Al_xGa_{1-x}As$. Our subsequent discussion showed how EBER spectra provide clear determinations of transition energies in quantum structures. In particular, our EBER

spectrum of a 50Å GaAs quantum and its corresponding theoretical fit were presented. We concluded with an examination of the experimental EBER spectrum of a HEMT device, demonstrating analysis of single heterojunction structures. These examples are indicative of the potential of EBER for advanced characterization of structured systems.

REFERENCES

1 Included in this group are the "first derivative" modulation spectroscopies of piezoreflectance (PzR), and thermoreflectance (TR), and the "third derivative" or electric field modulation spectroscopies of photoreflectance (PR), electrolyte electroreflectance (EER), surface barrier electroreflectance (SBER), and Electron Beam Electroreflectance (EBER). Previously EBER was described as "cathodoreflectance" in the literature.

2 See for example Semiconductors and Semimetals, Vol 9, edited by R. K. Willardson and A. C. Beer, (Academic Press, New York, 1972).

3 M. H. Herman and R. C. Bowman, Jr., (unpublished).

4 Monte Carlo simulations show that the 240eV electrons thermalize in most semiconductors within about 15Å of the surface.

5 The mechanism of EBER (cathodoreflectance) has been investigated by earlier researchers. See I. Broser, R.-A. Hoffman and H.-J. Schulz, Solid State Comm. 8, 587-591 (1970). See also J. H. McCoy and D. B. Wittry, Appl. Phys. Lett. 13(8), 272-274 (1968).

6 This has been found for both interband and excitonic transitions. For the excitonic case, see D. F. Blossey and P. Handler, in Semiconductors and Semimetals, Vol 9, edited by R. K. Willardson and A. C. Beer, (Academic Press, New York, 1972), p.257. The interband case is discussed by D. E. Aspnes, Surface Science 37, 418-442 (1973).

7 The PR mechanism has been substantiated by several groups. See for example E. Y. Wang and W. A. Albers, Physics Letters 27A(6), 347-348 (1968). D. E. Aspnes, Solid State Comm. 8, 267-270 (1970). F. Cardiera and M. Cardona, Solid State Comm. 7, 879-882 (1969).

8 M. H. Herman, R. L. Tober, and R. A. McFarlane (unpublished).

9 See for example J. W. Garland, and P. M. Raccah, SPIE 659, 32-43 (1986).

10 H. C. Casey and M. B. Panish, Heterostructure Lasers (Academic, New York, 1978), Part A, in S. Adachi, J. Appl. Phys. 1985, reprinted in Gallium Arsenide: Key papers in physics: no.1, edited by J. S. Blakemore, (American Institute of Physics, 1987), p.62.

11 U. K. Reddy, G. Ji, T. Henderson, H. Morkoc and J. N. Schulman, J. Appl. Phys. 62(1), 145-151 (1987).

12 M. H. Herman, S. E. Buttrill, Jr., G. L. Francke and F. A. Chambers, "Electron Beam Electroreflectance (EBER) analysis of single $Al_xGa_{1-x}As$/GaAs quantum wells," presented at the Electronic Materials Conference, June 1988, Boulder, Colorado (unpublished).

13 O. J. Glembocki, B. V. Shanabrook, N. Bottka, W. T. Beard, and J. Comas, Appl. Phys. Lett. 46(10), 970-2 (1985) and N. Bottka, D. K. Gaskill, R. S. Sillmon, R. Henry, and R. Glosser, J. Electr. Mater. 17(2), 161-170 (1988).

14 O. Aina, M. Mattingly, F. Y. Juan and P. K. Bhattacharya, Appl. Phys. Lett. 50(1), 43-45 (1987).

15 B. V. Shanabrook (private communication).

16 This factor is calculated by assuming the confined electrons have an infinite mass. Therefore, the Rydberg is increased by the ratio of the heavy hole mass to the usual interband reduced mass. The ionization field is proportional to the square of the reduced mass.